PASJ: Publ. Astron. Soc. Japan **57**, 815–820, 2005 October 25

Asymmetric Sub-Reflectors for Spherical Antennas and Interferometric Observations with an FPGA-Based Correlator

Hiroshi TAKEUCHI
Kashima Space Research Center, National Institute of Information and Communications Technology, 893-1 Hirai, Kashima, Ibaraki 314-8501
ht@nict.go.jp
Masaya KUNIYOSHI and Tsuneaki DAISHIDO
Department of Science, School of Education, Waseda University, 1-6-1 Nishi-Waseda, Shinjuku-ku, Tokyo 169-8050
Kuniyuki ASUMA
Kuki High School, 3-12-1 Honmachi, Kuki, Saitama 346-0005
Advanced Research Institute for Science and Engineering of Waseda University, 3-4-1 Okubo, Shinjuku-ku, Tokyo 169-8555
and
Nobuo MATSUMURA, Kazuhiro TAKEFUJI, Kotaro NIINUMA, Hajime ICHIKAWA, Riki OKUBO, Akihiro SAWANO, Naoya YOSHIMURA, Fumiyuki FUJII, Keiju MIZUNO, and Yukinori AKAMINE
Astrophysics, Department of Pure and Applied Physics, Graduate School of Science and Engineering, Waseda University, 3-4-1 Okubo, Shinjuku-ku, Tokyo 169-8555

(Received 2005 April 11; accepted 2005 July 30)

Abstract

The Nasu Radio Interferometer, consisting of eight equally spaced, 20-m diameter fixed spherical antennas, was developed for the purpose of surveying unknown variable radio sources at 1.4 GHz. An asymmetrical Gregorian sub-reflector was designed and installed on each antenna for the purpose of correcting aberrations caused by the spherical reflector. The total collecting area is $2512\,\mathrm{m}^2$ and the field-of-view of each antenna is $0.^\circ6 \times 0.^\circ6$. In survey observations a spatial-fast Fourier-transform (FFT)-type multi-beam system will be used. We report on the design of spherical reflectors and a digital back-end system, the basic principle of spatial-FFT image forming, and a result of interferometric observations with an FPGA-based digital correlator.

Key words: instrumentation: interferometers — radio continuum: general — techniques: interferometric

1. Introduction

The Nasu Radio Interferometer, located at Nishi-Nasuno, 160 km north of Tokyo, consists of eight equally spaced, 20-m diameter, fixed spherical antennas. Each antenna element is in a fixed position to obtain Nyquist-rate direct images using a real-time spatial fast Fourier-transform (FFT) processor, which was developed at the Waseda FFT interferometer (Daishido et al. 1991; Asuma et al. 1991). Since this direct-imaging method will be used for the Nasu Radio Interferometer, we give an outline of the Waseda FFT interferometer in section 2.

In fixed spherical reflectors, the construction costs is much less than that for the same size Cassegrain antennas. Instead, it requires a spherical aberration-correcting sub-reflector (Holt, Bouche 1964). In section 3, we consider the shape of the sub-reflector and describe the receiver system. In section 4, we report on some results of interferometric observations.

2. Spatial FFT Interferometer

Waseda University began constructing a spatial FFT interferometer in 1989, for surveying transient radio sources, such as Cyg X-3, Cir X-1, and supernovae. It consists of equally spaced two-dimensional 8×8 antennas. Each antenna element is a 2.4-m Cassegrain antenna, and the overall size of the array is $20\,\mathrm{m} \times 20\,\mathrm{m}$.

A two-dimensional spatial FFT processor is used for image formation. By the Nyquist-rate 2-dimensional spatial FFT of the signals from each antenna element, an 8×8 pixel image of the sky is obtained every 50 ns (Daishido et al. 1991; Nakajima et al. 1992, 1993). An example of the observed images with the FFT processor is shown in figure 1. The images show the transition of Tau A, by the diurnal motion of the earth, across the image plane of 8×8 pixels. Each pixel corresponds to a $0.^\circ078 \times 0.^\circ109$ region of sky.

This direct imaging method has the following features compared to Fourier synthesis:

- Fourier synthesis could map fine and precise source structures using a relatively small number of antennas by choosing minimum-redundant baselines or arbitrary configuration of antennas. The FFT interferometer, in which each antenna element is fixed in the maximum-redundant positions, generates rough images at the Nyquist rate.
- Wide-band observations have been achieved with a Fourier-synthesis interferometer, while multi-directional, relatively narrow-band observations at Nyquist rate are possible with the FFT interferometer.
- An N-element FFT interferometer requires only $N \log_2 N$ multipliers, while an N-element Fourier synthesis interferometer requires $N(N-1)$ correlators.

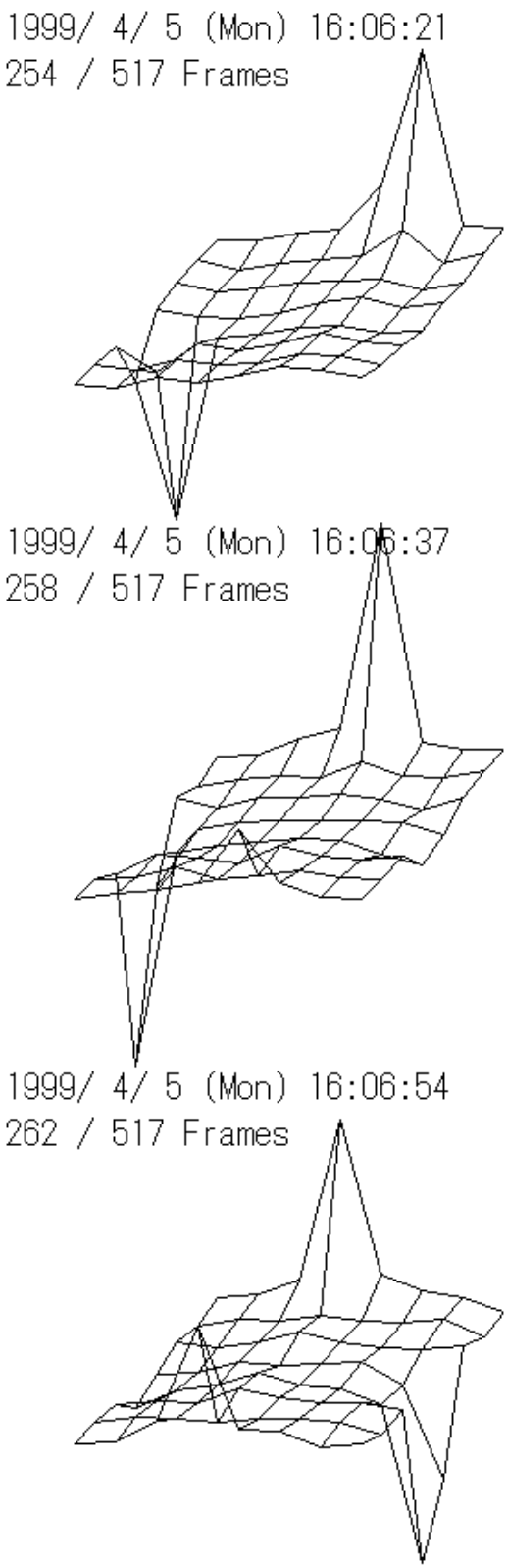

Fig. 1. Two-dimensional direct images of Tau A recorded at the Waseda FFT interferometer. These images were formed in real-time using a two-dimensional spatial FFT processor. The negative images appearing in these image planes are due to two-dimensional 180° phase switching.

If many elements are required, the implementation of FFT is easier than that of correlators.

- Fourier synthesis is applicable under the assumption that the brightness distribution of the sky is ergodic. On the other hand, FFT imaging can apply for non-ergodic sources, like pulsars or communication signals.

To obtain clean images with this FFT method, determining the antenna-based phase errors in the 64-analog transmission lines before the FFT observations is necessary. Because the antenna-based phase errors change, depending on the ambient temperature, phase calibrations should be performed a few times a day by observing strong calibrator sources during survey observations. The calibration algorithms have been improved progressively (Nakajima et al. 1993; Otobe et al. 1994; Takeuchi 2000), and the temperature dependence of phase errors has been reduced by replacing 50-m coaxial cables in IF transmission lines with digital optical fibers in 2000. In the present system, residual phase errors are limited to 5° (r.m.s.). This allows us to perform stable daily FFT observations. Routine survey observations have been performed, and daily variations in the radio intensity have been measured (Takeuchi et al. 2000).

The FFT processor was upgraded in 2001 so that it can perform 16×16 point spatial two-dimensional (2D) FFT and 256-point temporal one-dimensional FFT (Tanaka et al. 2000).

3. Design of Nasu Radio Interferometer

At the Nasu Radio Interferometer, a fixed spherical reflector is used for the main reflector of each antenna element, and asymmetrical Gregorian reflectors are used for the sub-reflectors. A photograph of the 20-m antennas is shown in figure 2. The radius of curvature and the aperture diameter are both 20 m, that is, it is a 60° spherical cap.

One of the disadvantages of fixed spherical reflector antennas is the narrowness of the observable sky region. It is limited to the region near the zenith because the effective aperture of the telescope is reduced at lower elevation angles. On the other hand, a fixed antenna has advantages in the costs for construction and maintenance, since there are fewer moving parts in fixed antennas than in the AZ–EL mount large antennas, and the surface curvature of spherical reflectors is constant everywhere. This is important when a large number of antennas are needed for a large collecting area. The construction cost per unit collecting area is about a hundredth of that for AZ–EL mounts. Taking into account the future extensibility of the number of antennas, fixed spherical reflector antennas were used for the array.

To make the antenna driving system simple and inexpensive, a transit-mount was used for the antennas. A sub-reflector and feed horn rotate synchronously around the vertical axis of the spherical reflector, on which both the phase center of the telescope and the center of the sphere are located (see figure 3). While an arbitrary azimuth angle is selectable by rotation, the elevation angle is fixed to 85° and cannot be changed. Therefore, tracking observations are not available, whereas drift-scan can be used for survey observations within a declination range of $36°55' \pm 5°$.

Fig. 2. Photograph of the array at Nasu Radio Interferometer. Eight equally spaced, 20-m diameter, fixed spherical antennas are shown in this figure.

3.1. Shape of Gregorian Sub-Reflector

Gregorian sub-reflectors are necessary as spherical aberration correctors for spherical reflectors. In this subsection, we discuss the shape of a sub-reflector using geometrical optics.

Consider the incoming ray from a celestial source with a zenith angle of ϕ. Assuming that the center of a sphere is identical to the origin of a coordinate system, the direction of the celestial source is parallel to the positive direction of the z-axis, and the focus of the reflector is in the y–z plane. The radius of the sphere is assumed to be 1, and the length between the origin and the focus $P(x_2, y_2, z_2)$ is set to p (see figure 4), which is

$$(x_2, y_2, z_2) = (0, p\sin\phi, -p\cos\phi). \tag{1}$$

Consider the first reflection at an arbitrary point (x_0, y_0, z_0) on the spherical main reflector. In figure 4, $\boldsymbol{n}$ represents the normal vector of the reflecting point, $\boldsymbol{i}$ a unit vector pointing in the direction of the incoming ray, and $\boldsymbol{r}$ a unit vector pointing in the direction of the reflected ray, that is

$$\boldsymbol{n} = -(x_0, y_0, z_0), \tag{2}$$

$$\boldsymbol{i} = (0, 0, -1). \tag{3}$$

From the law of reflection, $\boldsymbol{r}$ can be represented as

$$\begin{aligned}\boldsymbol{r} &= -(\boldsymbol{i}\cdot\boldsymbol{n})\boldsymbol{n} + \boldsymbol{i} - (\boldsymbol{i}\cdot\boldsymbol{n})\boldsymbol{n} \\ &= (2z_0x_0, 2z_0y_0, 2z_0^2 - 1).\end{aligned} \tag{4}$$

The coordinates of the second reflection point on the sub-reflector (x_1, y_1, z_1) can be expressed using the parameter t (> 0) as

$$\begin{aligned}(x_1, y_1, z_1) &= (x_0, y_0, z_0) + t\,\boldsymbol{r} \\ &= \left[(2tz_0 + 1)x_0, (2tz_0 + 1)y_0, (2tz_0 + 1)z_0 - t\right].\end{aligned} \tag{5}$$

Fig. 3. Photograph of a sub-reflector and horn antenna equipped with a 20-m spherical antenna. Both rotate synchronously around the vertex axis of the sphere. The elevation angle is fixed at 85°.

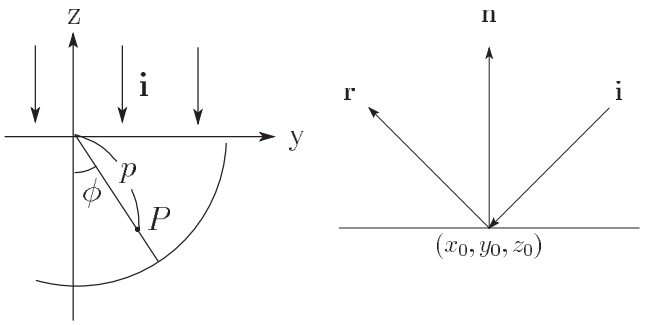

Fig. 4. Left: Cross-section in the y–z plane. Right: First reflection at an arbitrary point on the spherical main reflector.

We assume the length of the light path from the x–y plane to the main reflector is L_0, the length from the main reflector to the sub-reflector is L_1, and the length from the sub-reflector to the focus is L_2, which are given by

$$L_0 = -z_0, \tag{6}$$

$$L_1 = t, \tag{7}$$

$$L_2 = \sqrt{(x_1 - x_2)^2 + (y_1 - y_2)^2 + (z_1 - z_2)^2}. \tag{8}$$

Here, we define a free parameter, $L = L_0 + L_1 + L_2$, which represents the total length of the light path from the x–y plane to the focus, which is

$$(L + z_0 - t)^2 = (x_1 - x_2)^2 + (y_1 - y_2)^2 + (z_1 - z_2)^2. \tag{9}$$

Substituting equation (5) into equation (9), t can be given by

$$t = \frac{1 + p^2 - 2(y_0 y_2 + z_0 z_2) - (L + z_0)^2}{4z_0(y_0 y_2 + z_0 z_2) - 2(L + 2z_0 + z_2)}.$$

Considering the coordinates (X, Y, Z), in which the zenith corresponds to the Z-axis, the coordinates of arbitrary points on the spherical surface can be given with two parameters, (X_0, Y_0), by

$$\begin{pmatrix} x_0 \\ y_0 \\ z_0 \end{pmatrix} = \begin{pmatrix} 1 & 0 & 0 \\ 0 & \cos\phi & -\sin\phi \\ 0 & \sin\phi & \cos\phi \end{pmatrix} \begin{pmatrix} X_0 \\ Y_0 \\ -\sqrt{X_0^2 + Y_0^2} \end{pmatrix}. \tag{10}$$

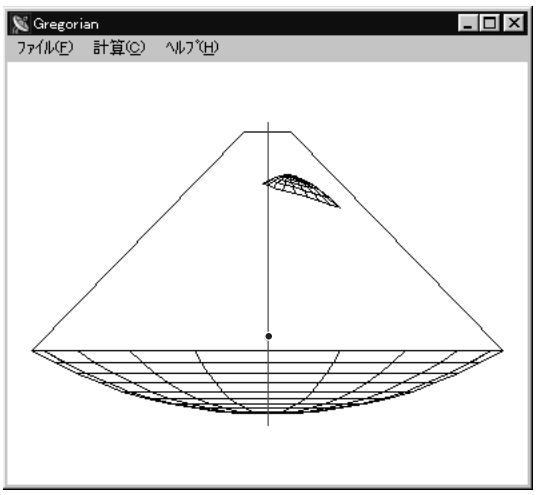

Fig. 5. Shape of a Gregorian sub-reflector with values of $p = 0.84$, $L = 0.93$, and $\phi = 5°$. The focal point is represented as a dot on the vertical axis.

To plot (x_1, y_1, z_1) by sweeping (X_0, Y_0) in the range of $X_0^2 + Y_0^2 < \sin 30°$, we can determine the three-dimensional shape of a sub-reflector using three parameters; p, L, ϕ. To generate a narrow beam, the current distribution on the aperture of the main reflectors should be as uniform as possible. The set of these parameters were calculated using ray-tracing programs for uniform illuminations in the aperture (Daishido et al. 2000; Takeuchi 2000). In figure 5, the shape of a Gregorian sub-reflector is displayed using the adopted values of $p = 0.84$, $L = 0.93$, and $\phi = 5°$.

3.2. *Back-End System*

A schematic diagram of the analog back-end system is shown in figure 6. To avoid radio interferences at the L-band, 20-MHz band-pass filters are used to limit the RF bandwidth to an allocated frequency band for radio astronomy. At a subsequent stage, RF signals are down converted to two orthogonal 10-MHz baseband signals, using complex mixers, and digitalized with A/D converters at the Nyquist rate (figure 7). The number of quantization bits is three.

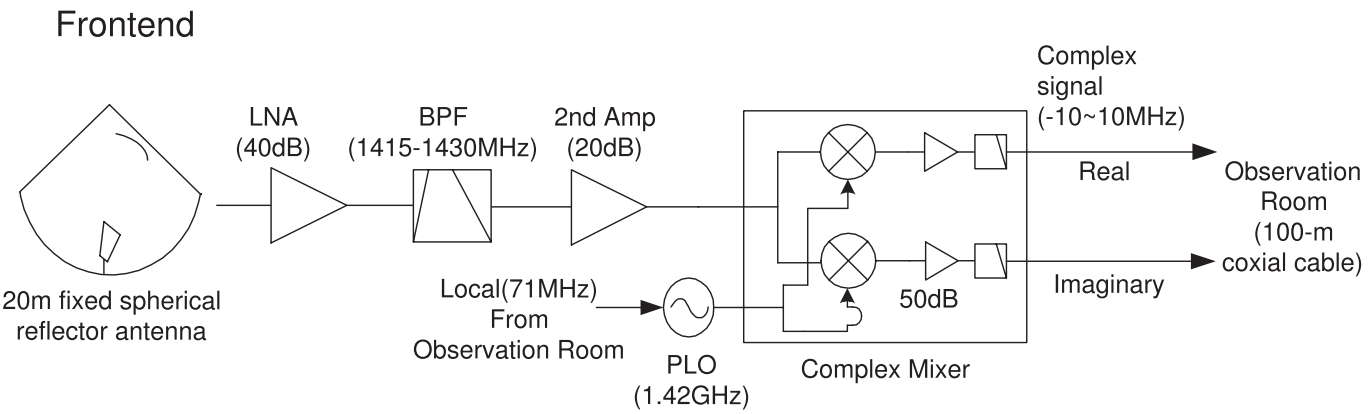

Fig. 6. Analog back-end system for each antenna element.

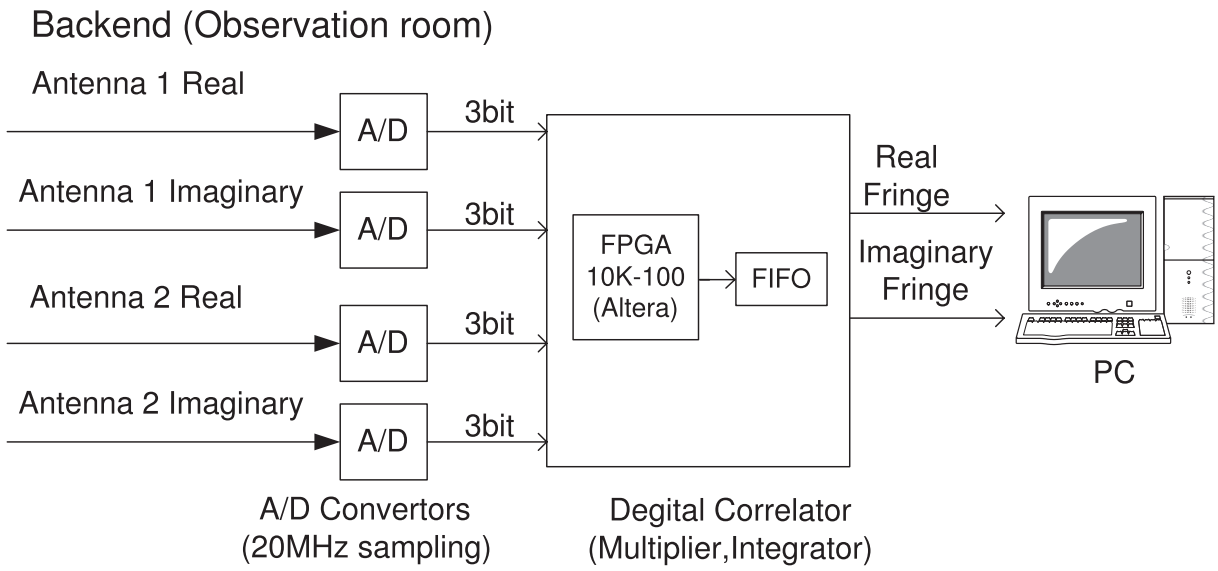

Fig. 7. Schematic diagram of the single-baseline digital correlator for the Nasu Radio Interferometer.

At the time of writing, a spatial FFT processor was used in the 8×8 Waseda interferometer. A simple single-baseline digital correlator with an FPGA 10K-100 (Altera corporation) was developed as well as analog correlators for basic interferometric observations. Using this digital correlator, complex signals from two antennas are multiplied at the Nyquist-rate and integrated for a minimum period of 800 μs. Multiplied data are then transmitted to a PC in real-time, and post analysis processes are performed in the PC.

4. Observations

Observations using the single-baseline digital correlator were made from 2002 December 21 to 29. The azimuth angle was fixed during the observation period toward a declination angle of $40^\circ 44'$. The baseline length was 22 m. The fringe signals of 3C 254 detected in the observations are shown in figure 8.

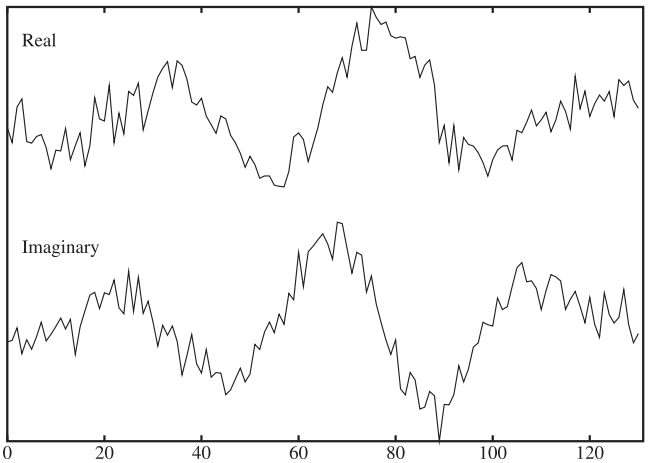

Fig. 8. Two orthogonal fringe components of 3C 254 (3.1 Jy at 1.4 GHz). Observed on 2002 December 21. The abscissa is time, and the integration time of each point is 4 s.

By comparing the signal-to-noise ratios of the fringe signals detected in the observations with the published 1.4-GHz radio catalog (White, Becker 1992), the minimum detectable flux density was estimated to be 0.3 Jy (1σ noise level, integration time 4 s, 20 MHz bandwidth).

5. Conclusion and Future Work

To perform wide-field survey observations, we developed an array consisting of eight 20-m spherical antennas. After the shape of asymmetric sub-reflectors was calculated, they were installed on each antenna for the purpose of correcting aberrations for the spherical reflectors. Continuous survey observations to monitor transient radio sources were started with analog correlators using four baselines simultaneously, and sensitive fringe fitting methods were developed. A basic single-baseline digital correlator discussed in this paper was also developed and used in 8 days of consecutive survey observations. We obtained a sensitivity of 0.3 Jy with 4 s integration time. For the next step, an FFT processor for the Nasu Radio Interferometer was also developed for multi-beam surveys. More sensitive survey observations are expected. In FFT processing, phase information is not lost and the system is adequate for multi-beam pulsar survey observations or in multi-directional communications.

References

Asuma, K., Iwase, S., Nishibori, K., Nakajima, J., Otobe, E., Tuchiya, A., Watanabe, N., & Daishido, T. 1991, in ASP Conf. Ser. 19, Proc. 131st IAU Colloq., ed. T. J. Cornwell & R. A. Parley (San Francisco: ASP), 90
Daishido, T., et al. 1991, in ASP Conf. Ser. 19, Proc. 131st IAU Colloq., ed. T. J. Cornwell & R. A. Parley (San Francisco: ASP), 86
Daishido, T., et al. 2000, Proc. SPIE, 4015, 73
Holt, F., & Bouche, E. 1964, IEEE Trans., Antennas Propagat., 12, 44
Nakajima, J., et al. 1993, PASJ, 45, 477
Nakajima, J., Otobe, E., Nishibori, K., Watanabe, N., Asuma, K., & Daishido, T. 1992, PASJ, 44, L35
Otobe, E., et al. 1994, PASJ, 46, 503
Takeuchi, H. 2000, PhD Thesis, Waseda University
Takeuchi, H., et al. 2000, PASJ, 52, 267
Tanaka, N., et al. 2000, PASJ, 52, 447
White, R. L., & Becker, R. H. 1992, ApJS, 79, 331